General Disclaimer

One or more of the Following Statements may affect this Document

- This document has been reproduced from the best copy furnished by the organizational source. It is being released in the interest of making available as much information as possible.

- This document may contain data, which exceeds the sheet parameters. It was furnished in this condition by the organizational source and is the best copy available.

- This document may contain tone-on-tone or color graphs, charts and/or pictures, which have been reproduced in black and white.

- This document is paginated as submitted by the original source.

- Portions of this document are not fully legible due to the historical nature of some of the material. However, it is the best reproduction available from the original submission.

NASA Technical Memorandum 74053

LOAD DISTRIBUTION ON A CLOSE-COUPLED WING CANARD AT TRANSONIC SPEEDS

By Blair B. Gloss and Karen E. Washburn

August 1977

National Aeronautics and
Space Administration

Langley Research Center
Hampton, Virginia 23665

LOAD DISTRIBUTION ON A CLOSE-COUPLED WING CANARD AT TRANSONIC SPEEDS

Blair B. Gloss and Karen E. Washburn+
NASA Langley Research Center
Hampton, Virginia 23665

Abstract

This paper reports on a wind-tunnel test where load distributions were obtained at transonic speeds on both the canard and wing surfaces of a closely-coupled wing-canard configuration. The investigation included detailed component and configuration arrangement studies to provide insight into the various aerodynamic interference effects for the leading-edge vortex flow conditions encountered. Data indicate that increasing the Mach number from 0.70 to 0.95 caused the wing leading-edge vortex to burst over the wing when the wing was in the presence of the high canard. For some of the outboard span locations, the leading-edge vortex reattachment streamline intersects the wing trailing edge inboard of these span locations, thus, the Kutta condition was not satisfied. In general, the effect of adding a canard was to reduce the lift inboard and somewhat increase the lift outboard similar to the trends that would have been expected had the flow been attached.

Symbols

b	model semispan, cm
b^*	exposed wing semispan, cm
c	local chord, cm
c_{avg}	average chord length, cm
$\bar{c}$	mean geometric chord, cm
c_r	chord length at fuselage-wing juncture
c_n	section normal force coefficient
$C_{L,W}$	lift on aft body and wing (Ref. 4)
C_p	pressure coefficient
C_p^*	sonic pressure coefficient
ΔC_p	C_p upper surface - C_p lower surface
$(\Delta C_p)_c$	ΔC_p canard on - ΔC_p canard off
M	Mach number
S	wing reference area (wing extended to model center line), cm^2
x	longitudinal distance, cm
y'	lateral distance - measured from wing-fuselage intersection, cm
z	height above mid-chord plane of model, cm
α	angle of attack, deg
Λ	leading edge sweep, deg
Λ_{isobar}	isobar sweep, deg
η	y'/b^*
γ	ratio of specific heats

Introduction

Past investigations (Refs. 1-13) have indicated that the proper use of canard surfaces on maneuvering aircraft can offer several attractive features such as potentially higher trimmed-lift capability, improved pitching moment characteristics and reduced trimmed drag. In addition, the geometric characteristics of close-coupled canard configurations offer a potential for improved longitudinal progression of cross-sectional area which could result in reduced wave drag at low supersonic speeds and placement of the horizontal control surfaces out of the high wing down wash and jet exhaust. Flow visualization studies (Ref. 13) and analytical studies (Refs. 14 and 15) have indicated that the favorable interference of the canard on the wing's lift produces a complex flow field on the wing surface. Although there have been several papers published discussing the total forces and moments produced by close-coupled canard-wing configurations, very little data is available on the load distribution on canard and wing surfaces for close-coupled canard wing configurations.

This paper reports on a wind-tunnel investigation where load distributions were measured at transonic speeds on both the canard and wing surfaces of a closely-coupled wing-canard configuration. The investigation included detailed component and configuration arrangement studies to provide insight into the various aerodynamic interference effects. In addition to the detailed pressure measurements, the pressures have been integrated to illustrate the effects of Mach number, canard location, and canard-wing interference effects on various aerodynamic parameters. The present investigation was conducted in the Langley 8-foot transonic pressure tunnel; the Mach numbers ranged from 0.70 to 1.20 and data was taken from 0^o to approximately 20^o angle of attack.

Description of Model

A drawing of the model used in the wind-tunnel test (discussed in this paper) is presented in Figure 1. This model was designed so that various wing and canard planforms could be attached to the common fuselage and the positional relationship of the lifting surfaces (canards and wings) could also be varied. The wings and canards were instrumented with several pressure

+AIAA Student Member

orifices; the upper surface orifices were located on one lifting surface (wing or canard) and the lower surface orifices were located on the lifting surface on the other side of the model. However, both the instrumented canards and instrumented wings could not be tested simultaneously because of space restrictions in the model; thus, when both the canards and wings were on the model at the same time either the wings or canards were uninstrumented. Table I presents the pertinent geometric parameters associated with this model.

The 60^{o} swept untwisted wing had uncambered circular-arc airfoil sections and maximum thickness which varied linearly from 6 percent of the chord at the root (the root in this paper is the intersection of the fuselage and wing) to 4 percent of the chord at the tip.

The canard had a leading-edge sweep angle of 51.7^{o} and an exposed area of 28.0 percent of the wing reference area S. The canard was tested in the chord plane of the wing ($z/\bar{c} = 0.0$) and in positions 18.5 percent of the wing mean geometric chord above and below the wing chord plane ($z/\bar{c} = 0.185$ and -0.185). To obtain the configuration with the canard located below the wing chord plane, the model with the canard in the high position was rolled 180^{o} on the sting. The canard was untwisted and had uncambered circular-arc airfoil sections. The maximum thickness varied linearly from 6 percent of the chord at the root to 4 percent at the tip.

Results and Discussion

Although load distributions were obtained on both the canard and wing surfaces, this paper will focus on only the wing loads since the wing-canard interference effects are more pronounced on the wing. All the data presented will be for a nominal angle of attack of approximately 12.7^{o}; the exact angle of attack for each configuration discussed is shown in Table II.

Aerodynamic Force Characteristics

Because of the sharp leading edge and relatively high sweep of the wing, the aerodynamic forces are characterized to various degrees by the well known leading-edge vortex flow. To illustrate the effect on the aerodynamic forces and to provide background information related to the pressure results, some of the force results presented in Reference 4, obtained on a geometrically identical model are presented herein. The wind-tunnel model discussed in Reference 4 was instrumented with two strain gage balances, as shown in Figure 2; one balance measured the load on the forebody and canards while the other balance measured the total load on the model. Figure 3 shows the effect of Mach number on wing lift, $C_{L,W}$, ($C_{L,W}$ is the difference between the lift on the main balance and the lift on the canard balance, see Figure 2) for the high canard configurations. In this paper, the high canard is located at $z/\bar{c} = 0.185$; mid-canard at $z/\bar{c} = 0.0$ and low canard at $z/\bar{c} = -0.185$.

The data in Figure 3 show there are only small effects of Mach number on the total lift as would be expected from the relatively high sweep angles. The effect of canard location on wing lift is shown in Figure 4. These data indicate that the canard downwash substantially reduces the wing lift over the angle-of-attack range shown. In general, the low canard reduces the lift on the wing the most and the high canard the least. It can be seen in Figure 4 that for the Mach number 0.95 case, the wing not in the presence of the canard appears to stall, the leading-edge vortex bursts over the wing at some angle of attack greater than 12^{o}, while the wing in the presence of the canards show no sign of wing stall. To indicate some of the problems involved with predicting the total load versus angle of attack for a wing in the presence of a canard, Figure 5 shows a comparison of experimental and theoretical wing lift. On the left, the data is compared with potential flow theory and on the right with vortex lift theory. Since the wing is swept 60^{o} and produces a separation induced leading-edge vortex, the under prediction of lift using potential flow theory should be expected for both the wing in the presence of the canard and the wing alone configurations. It is of interest to note, however, that with the wing in the presence of the canard, the increase in wing lift over potential flow theory is much greater and at high angles of attack nearly offsets the downwash effect from the canard. The vortex lift theory agrees well with experiment for the wing alone case up to an angle of attack of approximately 13 degrees where the leading-edge vortex appears to burst in the vicinity of the wing. However, for the wing in the presence of the canard, no breakdown effect is evident and the lift exceeds that predicted by the vortex lift theory. It is assumed that the additional vortex lift implied by the comparison may be associated with a stablizing effect on and possibly an augmentation of the wing leading-edge vortex by the canard flow field.

Effect of Mach Number on Wing Loads in the Presence of a Canard

Mach numbers 0.70 and 0.95 chordwise pressure distribution data on the wing for the high canard configuration is shown in Figure 6. Since this model has sharp leading-edged wings and the leading edge is swept 60^{o}, a leading-edge vortex is expected to form as discussed above. The chordwise pressure distribution for the 0.70 Mach number case indicates there is a leading-edge vortex which washes back over the wing; however, the 0.95 Mach number case indicates a leading-edge vortex inboard and there appears that there may be a vortex washing back over the wing, but these data are not conclusive. In the span region of $\eta = .82$, it is seen that the Kutta condition tends not to be satisfied for either Mach number. For a further understanding of the flow field on the wing at these Mach numbers, Figures 7 and 8 show isobars on the wing in the presence of the high canard and with the canard removed for Mach numbers of 0.70 and 0.95.

For the Mach number 0.70 case, the flow appears to be everywhere subcritical, since the critical pressure coefficient for 0.70 Mach number is approximately -1.23, as calculated by equation (1) for an isobar swept 60°.

$$C_p^* = \frac{2}{\gamma M^2}\left\{\left[\frac{2}{\gamma+1}\left(1+\frac{\gamma-1}{2}M^2(\cos\Lambda_{isobar})^2\right)\right]^{\frac{\gamma}{\gamma-1}}-1\right\} \quad (1)$$

The isobars in Figure 7 are swept more than 60° so the C_p^* would be something less than the -1.23 value cited above. The path of the leading-edge vortex over the upper surface of the wing is evident in Figure 7. The pressure distributions shown in Figure 6 for the spanwise location of $\eta = .82$ indicates that the Kutta condition is not satisfied for the Mach number 0.70 case. The isobars in Figure 7 indicate that the vortex induced reattachment line intersects the wing trailing edge inboard of the $\eta = .82$ station; thus, the Kutta condition would not be expected to be satisfied. It seems likely from the data in Figure 7 that the wing tip is stalled.

The isobars for the 0.95 Mach number case, Figure 8, appear to be a good deal more complicated than the 0.70 Mach number case. For isobars swept 66°, which is a nominal sweep for the isobars shown in Figure 8, the critical pressure coefficient (C_p^*) becomes approximately -0.67 and for no sweep of the isobars C_p^* becomes -0.09. The data in Figures 6 and 8 indicate that there is a shock wave which runs generally as the isobars run in the leading-edge section of the wing out to a span station of $\eta = .35$. Further outboard, the isobars tend to be unswept, thus, the flow on the upper surface of the wing outboard of an η of approximately .35 is supersonic. The $C_p = -.95$ isobar closes on itself in the vicinity of $\eta = .71$. It is suggested that the vortex has burst here causing a rapid growth in the vortex core size, and the separation bubble is seen. The reattachment line appears to be off the wing surface, thus, causing the Kutta condition to be unsatisfied. Even though the vortex has burst, it is felt there is still circulation around the vortex, and the far field flow, above the wing, is still organized. This seems reasonable since as is seen in Figure 3, the total lift on the wing for the 0.95 Mach number shows little indication of loss of lift due to vortex bursting. Thus, it appears that there is a wing leading-edge vortex passing over the wing at Mach number of 0.95, but the vortex bursts over the wing and, comparing Figures 7 and 8, the vortex appears to be pulled somewhat forward on the aft portion of the wing. It is felt, based on the 0.95 and 0.70 Mach number data, that if the canard semispan were the same as the wing semispan further gains could be made in the wing performance.

The effect of Mach number on the span load distribution is shown in Figure 9 for the wing in the presence of the high canard. The span loads seem to correlate well with the total loads shown in Figure 3. In the description of the model, it was pointed out that the wing was uncambered and untwisted with a sharp leading edge, thus, optimum span loads, as regards induced drag, should not be expected. Integrating these loads, in Figure 9, yields the center of pressure locations shown in Figure 10 for the wing in the presence of the high canard at three Mach numbers. As might be expected, there is a rearward movement of center of pressure with Mach number; this rearward movement is approximately 5 percent of the mean geometric chord of the wing. It is interesting to note that although there is substantial differences in the character of flow in going from a Mach number of 0.70 to 0.95 (Figs. 6, 7, and 8), there is essentially no spanwise movement of the center of pressure.

Effect of Canard Location on Wing Loads

In order to help explain some of the pressure distribution results that will be presented in this section, a brief discussion of some of the flow visualization results of Reference 13 is in order. These flow pictures indicate that for the high and mid-canard positions, the canard wake is well above the wing upper surface for an angle of attack of 12.7°; thus, although induced effects can occur, the canard wake does not physically interfere with the wing for these two configurations at this angle of attack. However, the flow pictures of Reference 13 indicate that the wing is in the wake of the low canard much of the time; therefore, since the wing is in this low energy wake, it is expected that the wing in the presence of a low canard will lose substantial lift.

Chordwise pressure distributions

Chordwise pressure distributions at two spanwise stations, $\eta = .24$ and .71, are shown in Figures 11 and 12 for the wing in the presence of the high canard and wing alone at two Mach numbers, 0.70 and 0.95. For both Mach numbers, the effect of the canard downwash at the inboard station, $\eta = .24$, on both the upper and lower surfaces is, of course, to reduce the effective angle of attack of this station. In addition to apparently weakening the strength of the leading-edge vortex of the wing at this inboard station, the interference of the canard on the wing moves the leading-edge vortex forward. At the outboard station, $\eta = .71$, there is evidence of the leading-edge vortex passing over a rather aft chordwise location for both Mach numbers for the canard on configuration; while, for the canard off configuration, there is little evidence of a vortex at the $\eta = 0.71$ span station. Although the Kutta condition is not satisfied at the $\eta = 0.71$ station for the canard off configuration, the data seem to indicate that this particular section is stalled rather than the vortex reattachment line intersecting the wing trailing edge inboard of the $\eta = .71$ station. The isobar plots in Figures 7 and 8 show a little more graphically that the effect of the canard interference is to move the leading-edge vortex forward and improve the flow on the outboard sections of the wing. Thus, even with leading-edge vortex flow, the net effect of the canard is to decrease the load inboard and increase the load outboard as would be expected with attached flow.

Since, for the mid-canard configuration, the canard wake is located physically closer to the wing than for the high canard configuration, stronger effects of canard downwash on the wing should be expected for, at least, the inboard wing stations. Figures 13 and 14 shows that this speculation is correct; the pressure distributions at span station η = .24, show a much stronger effect of canard downwash on the wing pressure distribution for the mid-canard than for the high canard. In fact, as mentioned earlier, for the high canard configuration, there appeared to be a shock located at the η = 0.24 span station at a Mach number of 0.95, but the downwash of the canard on the wing appears to have suppressed the shock at a Mach number of .95 for the mid-canard configuration (C_p*, @ Λ_{isobar} = 66°, = -.67). As with the high canard configuration, the interference effects of the canard on the wing appears to enhance the vortex at the outboard station, η = .71. Again, as discussed earlier, the vortex reattachment streamline intersects the wing trailing edge inboard of the η = .71 station and, thus, the Kutta condition is not satisfied.

The effect of the interference of the low canard on the inboard station, η = .24, completely changes the character of the pressure distribution from what had occurred for the high and mid-canard configurations, Figures 15 and 16. From the flow visualization pictures presented in Reference 13, this rather drastic change in pressure distribution appears to be due to the wake of the canard physically interacting with the wing. The outboard station appears to be very similar to the other two configurations.

A summary of the effect of canard position on wing lifting pressure for a Mach number of 0.70 is shown in Figure 17. As should be expected from the earlier discussion, it is seen that for the inboard sections, the canard affects the front portion of the wing while outboard, the largest effects of canard are on the aft portion of the wing. Using these results in Figure 17, Figure 18 presents a plot comparing attached flow theory with experiment plotted in the difference between lifting pressure for canard on and canard off. Of course, attached flow theory should not be expected to agree well with the experiment since the flow is separated for this model. However, in the absence of any better theory, the attached flow theory is presented. The theory, of course, thus, misses the vortex on both the inboard and outboard sections. The data in Figure 18 does show the magnitude of the error incurred when potential flow theory is used to compute the canard interference effect on the wing when the wing has a leading-edge vortex and emphasizes the need for loads prediction methods that accurately account for vortex flows.

The effect of canard location at Mach numbers of .70 and .95 on the span load distribution is presented in Figure 19. In general, it is seen that on the inboard section of the wing, the low canard configuration loses the most lift and the high canard the least. While on the outboard section of the wing, all three canard configurations produce more lift than the canard off configuration. This is due to the enhanced leading-edge vortex passing over this section of the wing for the canard configurations.

Figure 20 shows the center of pressure location for each chordwise station plotted for the canard off configuration and the three canard configurations. There is little effect of the canard on the outboard sectional center of pressures. However, for the wing inboard stations, moving the canard from the high position to low moves the center of pressure rearward for both Mach numbers shown. Further integration of the span load distributions yields the total center of pressure, as is shown in Figure 21 for Mach numbers 0.70 and 0.95. The effect of adding a canard to the wing load is to move the center of pressure rearward and outward.

Concluding Remarks

The effect of placing a relatively highly swept wing (Λ = 60°) having leading-edge vortex flow in the presence of a canard located above, in and below the wing chord plane on the wing load distribution has been determined at transonic speeds. The results, illustrated by data at an angle of attack of 12.7° indicate that increasing the Mach number from 0.70 to 0.95 caused the wing leading-edge vortex to burst over the wing when the wing was in the presence of the high canard. For some of the outboard span locations, the Kutta condition was not satisfied since the leading-edge vortex reattachment line intersected the wing trailing edge inboard of these span stations. In general, the effect of adding a canard was to reduce the lift inboard on the wing and somewhat increase the lift outboard similar to the trends that would have been expected had the flow been attached.

References

[1]McKinney, Linwood W.; and Dollyhigh, Samuel M.: Some Trim Drag Considerations for Maneuvering Aircraft. J. Aircraft, vol. 8, no. 8, Aug. 1971, pp. 623-629.

[2]Dollyhigh, Samuel M.: Static Longitudinal Aerodynamic Characteristics of Close-Coupled Wing-Canard Configurations at Mach Numbers From 1.60 to 2.86. NASA TN D-6597.

[3]Gloss, Blair B.; and McKinney, Linwood W.: Canard-Wing Lift Interference Related to Maneuvering Aircraft at Subsonic Speeds. NASA TM X-2897, 1973.

[4]Gloss, Blair B.: Effect of Canard Height and Size on Canard-Wing Interference and Aerodynamic Center Shift Related to Maneuvering Aircraft at Transonic Speeds. NASA TN D-7505, 1974.

[5]Gloss, Blair B.: The Effect of Canard Leading-Edge Sweep and Dihedral Angle on the Longitudinal and Lateral Aerodynamic Characteristics of a Close-Coupled Canard Wing Configuration. NASA TN D-7814.

[6]Gloss, Blair B.: Effect of Wing Planform and Canard Location and Geometry on the Longitudinal Aerodynamic Characteristics of a Close-Coupled Canard Wing Model at Subsonic Speeds. NASA TN D-7910.

[7]Behrbohm, Hermannn: Basic Low Speed Aerodynamics of the Short-Coupled Canard Configuration of Small Aspect Ratio. SAAB TN-60 Saab Aircraft Co. (Linkoping, Sweden), July 1965.

[8]Lacey, David W.; and Chorney, Stephen J.: Subsonic Aerodynamic Characteristics of Close-Coupled Canards With Varying Area and Position Relative to a 50° Swept Wing. Tech. Note AL-199 Naval Ship Res. & Develop. Center. March 1971.

[9]Ottensoser, Jonah: Wind Tunnel Data on the Transonic Aerodynamic Characteristics of Close-Coupled Canards With Varying Planform Position and Deflection Relative to a 50° Swept Wing. Test Rep. AL-88, Naval Ship Res. & Develop. Center, May 1972.

[10]Krouse, John R.: Effects of Canard Planform on the Subsonic Aerodynamic Characteristics of a 25° and a 50° Swept Wing Research Aircraft Model. Evaluation Rep. AL-91, Naval Ship Res. & Develop. Center, Aug. 1972.

[11]Lacey, David W.: Transonic Characteristics of Close-Coupled Canard and Horizontal Tail Installed on a 50 Degree Sweep Research Aircraft Model. Evaluation Rep. AL-8 Naval Ship Res. and Develop. Center, Aug. 1972.

[12]Gloss, Blair B.; Henderson, William P.; and Huffman, Jarrett K.: Effect of Canard Position and Wing Leading-Edge Flap Deflection on Wing Buffet at Transonic Speeds. NASA TM X-72681, 1975.

[13]Miner, Dennis D.; and Gloss, Blair B.: Flow Visualization Study of Close-Coupled Canard-Wing and Strake-Wing Configuration. NASA TM X-72668, 1975.

[14]Lamar, John E. and Gloss, Blair B.: Subsonic Aerodynamic Characteristics of Interacting Surfaces With Separated Flow Around Sharp Edges Predicted by a Vortex-Lattice Method. NASA TN D-7921, 1975.

[15]Lamar, John E.: Some Recent Applications of the Suction Analogy to Vortex-Lift Estimates. NASA TM X-72785, 1976

TABLE I.- Geometric Characteristics

	Wing	Canard
b - cm	25.4	17.25
b* - cm	21.6	13.4
Λ - deg	60	51.7
Airfoil section	Circular arc	Circular arc
S (wing area extended to plane of symmetry) cm^2	1032.2	----
Root chord (wing-body juncture) cm	29.8	17.92
Tip chord - cm	6.77	3.59
Maximum thickness, percent chord, at -		
Root	6	6
Tip	4	4

TABLE II.- Configuration Angle of Attack

Configuration	α, deg (M = .70)	α, deg (M = .95)	α, deg (M = 1.20)
High canard:			
canard on	12.67	12.97	13.06
canard off	12.30	12.39	----
Mid canard:			
canard on	12.63	12.89	----
canard off	12.27	12.33	----
Low canard:			
canard on	12.55	12.73	----
canard off	12.31	12.38	----

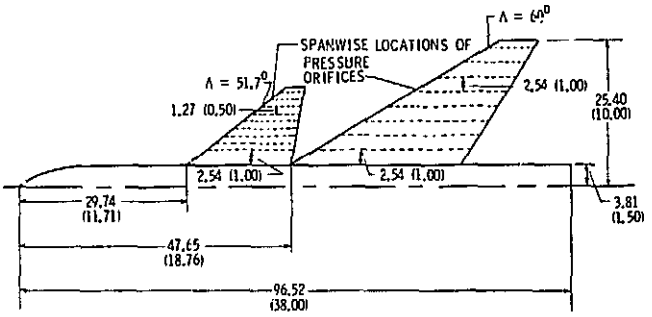

Figure 1. Sketch of pressure model, dimensions in centimeter (inches).

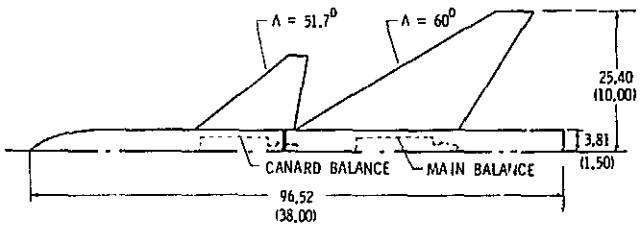

Figure 2. Planform view of strain gage instrumented model, reference 4.

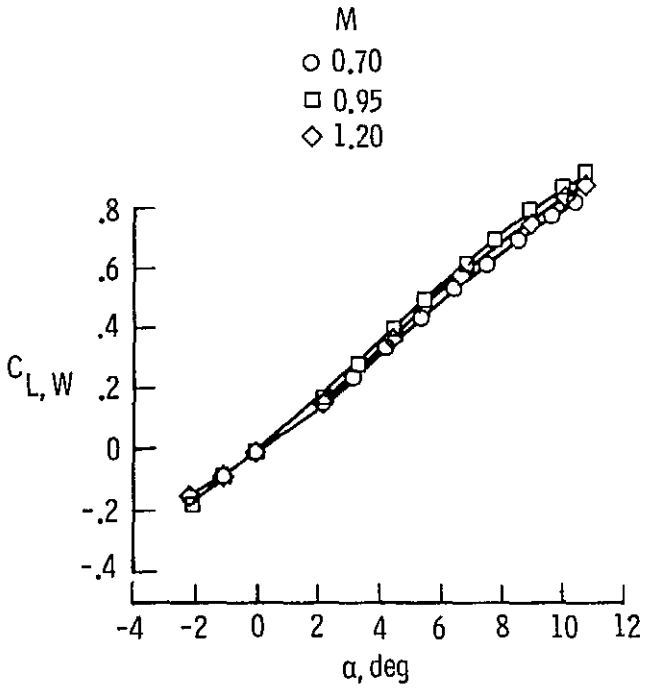

Figure 3. Effect of Mach number on wing lift for the high canard configuration, reference 4.

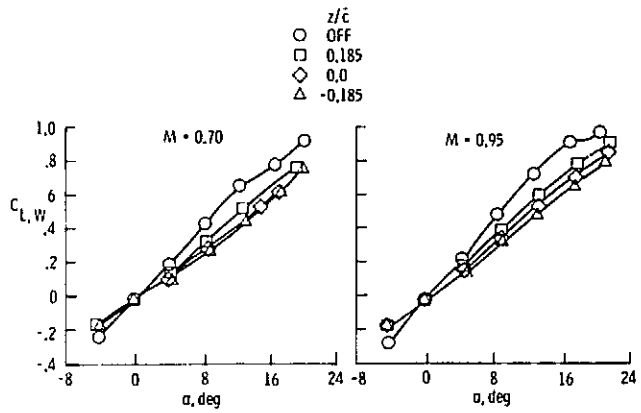

Figure 4. Interference effect of the canard on wing lift, reference 4.

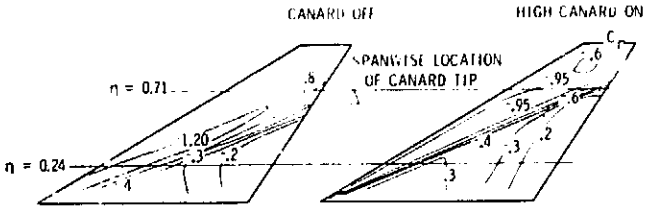

Figure 7. Lines of constant pressure for canard off and high canard on, M = 0.70.

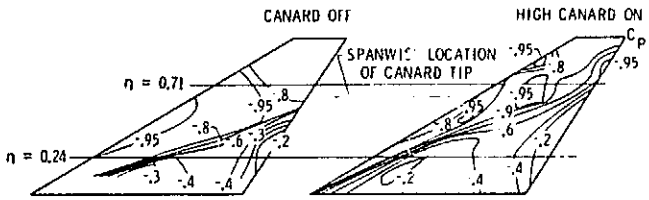

Figure 8. Lines of constant pressure for canard off and high canard on, M = 0.95.

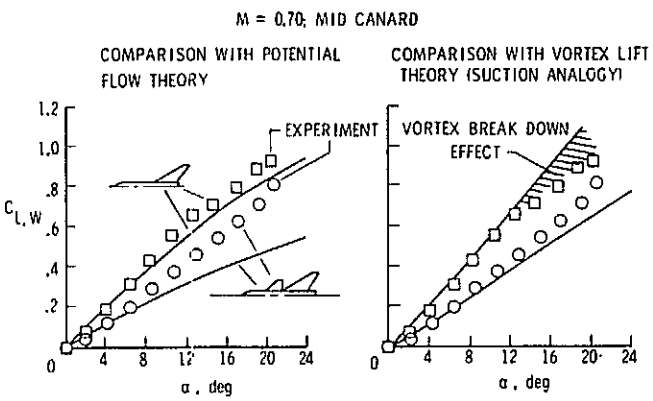

Figure 5. Comparison of experimental and theoretical canard interference effect on wing lift, M = 0.70, reference 4.

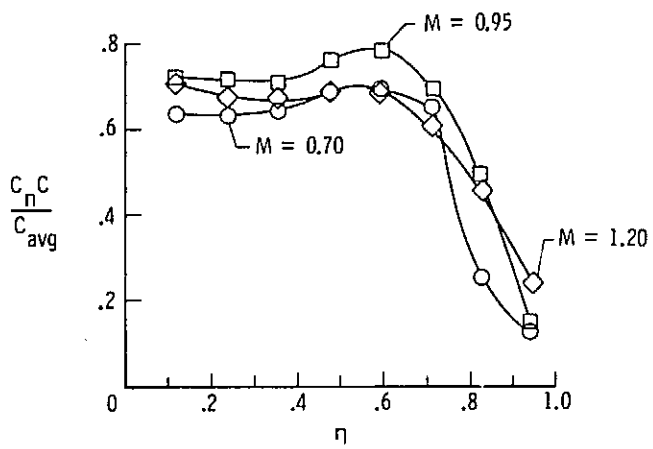

Figure 9. Effect of Mach number on spanload distribution for the high canard configuration.

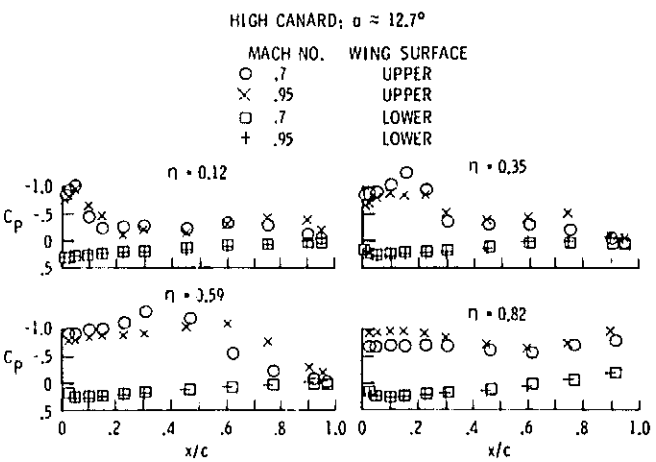

Figure 6. Chordwise pressure distribution for the high canard configuration.

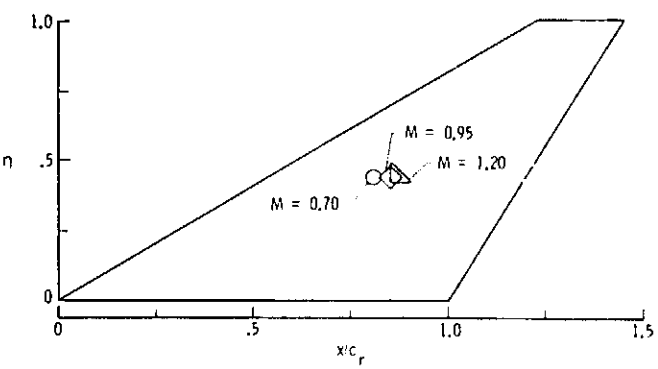

Figure 10. Effect of Mach number on center of pressure location, high canard configuration.

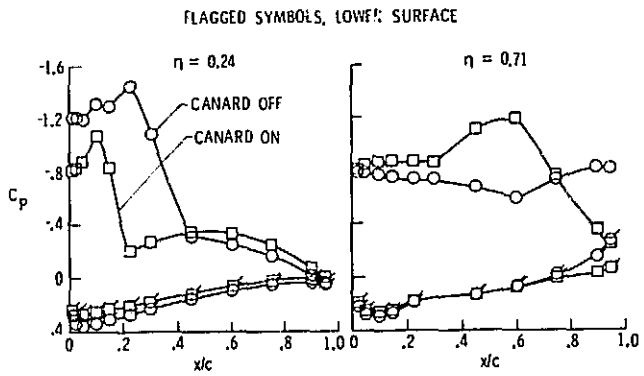

Figure 11. Wing chordwise pressure, distributions from the high canard configuration at a Mach number of 0.70.

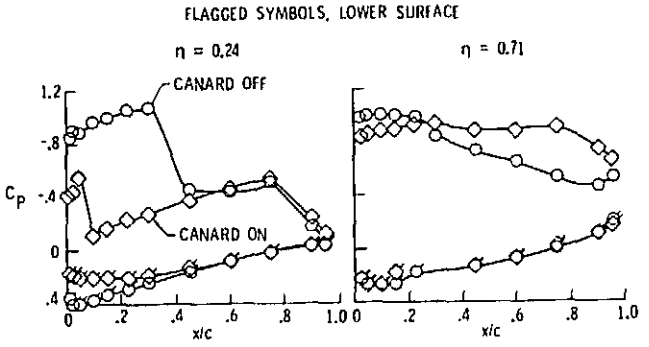

Figure 14. Wing chordwise pressure distribution for the mid-canard configuration at a Mach number of 0.95.

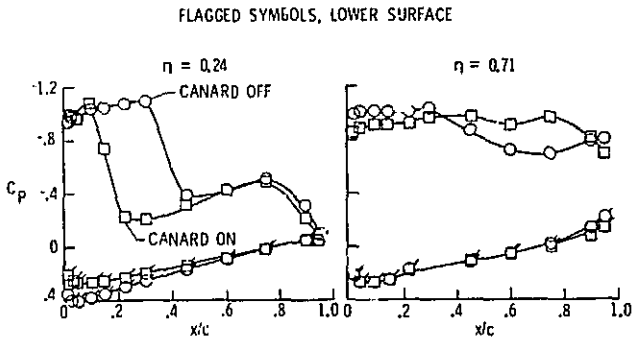

Figure 12. Wing chordwise pressure distribution for the high canard configuration at a Mach number of 0.95.

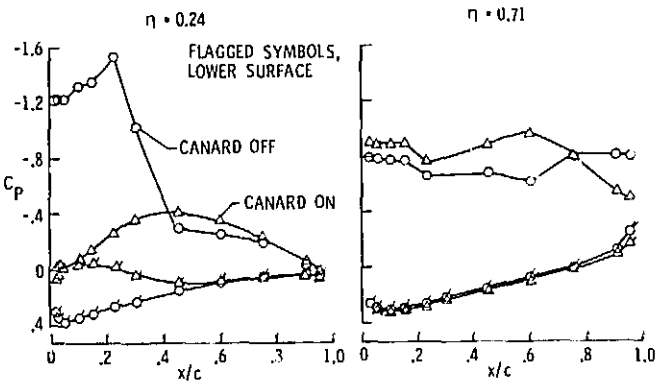

Figure 15. Wing chordwise pressure distribution for the low canard configuration at a Mach number of 0.70.

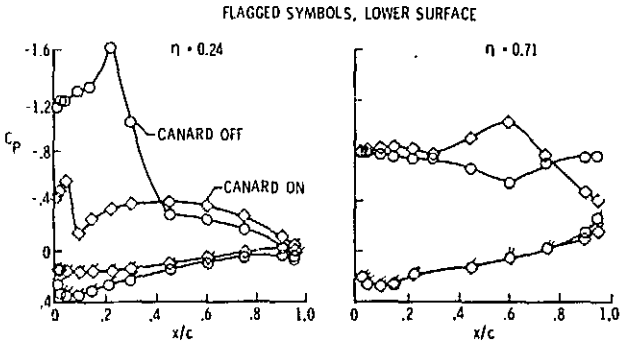

Figure 13. Wing chordwise pressure distribution for the mid-canard configuration at a Mach number of 0.70.

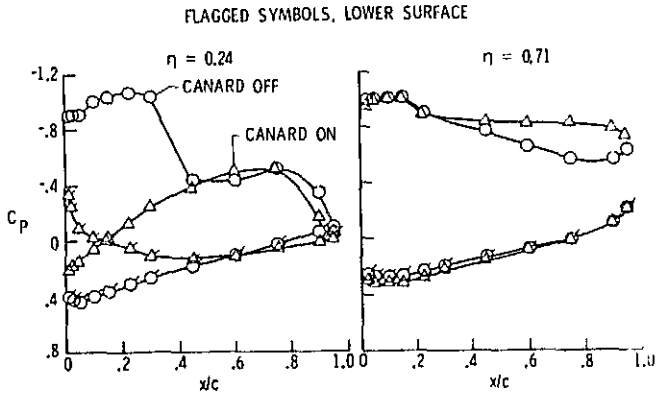

Figure 16. Wing chordwise pressure distribution for the low canard configuration at a Mach number of 0.95.

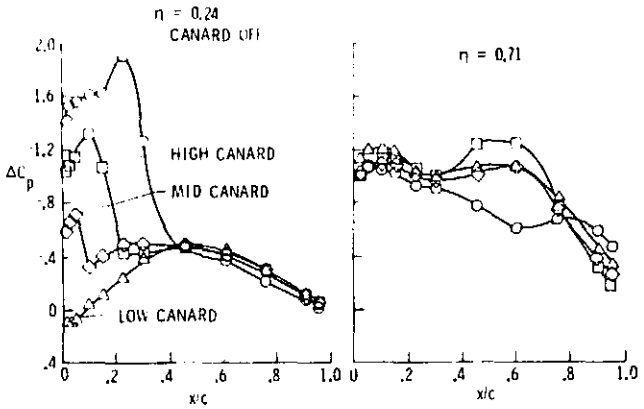

Figure 17. Effect of canard location on wing lifting pressure, Mach number equals 0.70.

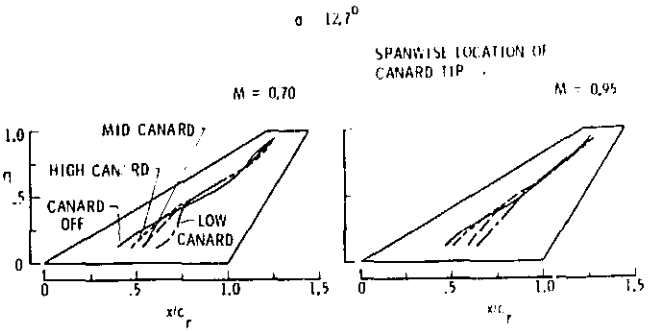

Figure 20. Effect of canard location on sectional center of pressure location.

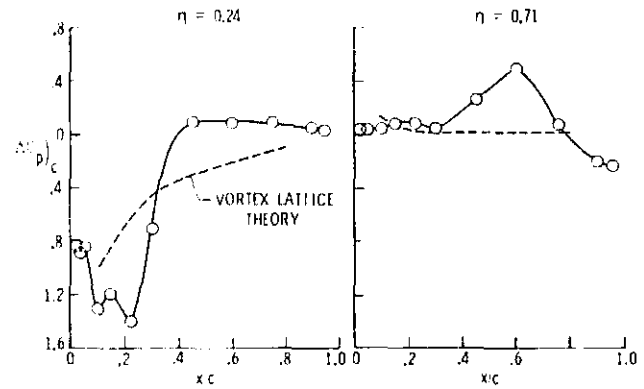

Figure 18. Effect of canard on wing lifting pressure for the mid-canard at a Mach number of 0.70.

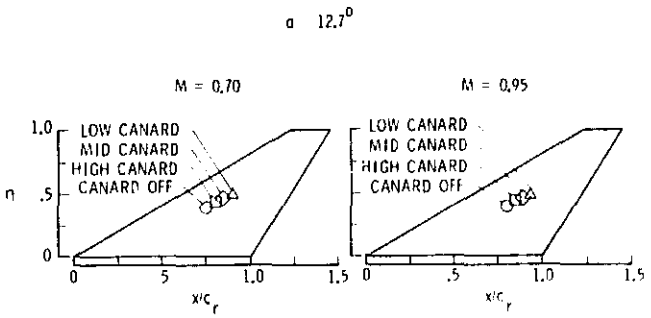

Figure 21. Effect of canard location on center of pressure location.

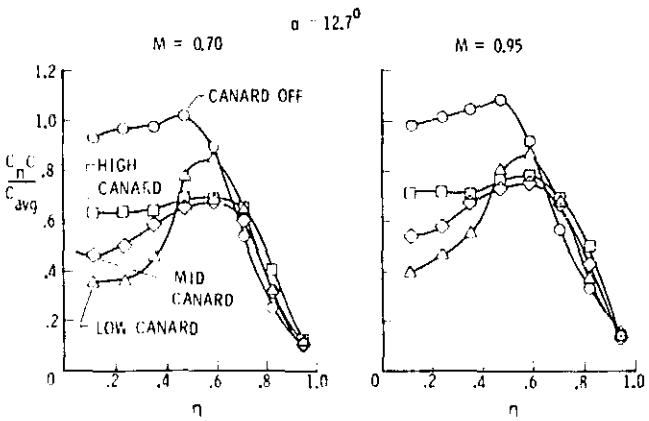

Figure 19. Effect of canard location on wing spanload distribution.

1. Report No.	2. Government Accession No.	3. Recipient's Catalog No.
NASA TM 74053		

4. Title and Subtitle	5. Report Date
LOAD DISTRIBUTION ON A CLOSE-COUPLED WING CANARD AT TRANSONIC SPEEDS	August 1977
	6. Performing Organization Code
7. Author(s)	8. Performing Organization Report No.
Blair B. Gloss and Karen E. Washburn	
	10. Work Unit No.
9. Performing Organization Name and Address	505-11-21-02
NASA Langley Research Center Hampton, Virginia 23665	11. Contract or Grant No.
	13. Type of Report and Period Covered
12. Sponsoring Agency Name and Address	
National Aeronautics and Space Administration Washington, DC 20546	14. Sponsoring Agency Code

15. Supplementary Notes

Presented at the AIAA Fourth Atmospheric Flight Mechanics Conference, Hollywood, Florida, August 8-10, 1977.

16. Abstract

This paper reports on a wind-tunnel test where load distributions were obtained at transonic speeds on both the canard and wing surfaces of a closely-coupled wing-canard configuration. The investigation included detailed component and configuration arrangement studies to provide insight into the various aerodynamic interference effects for the leading-edge vortex flow conditions encountered. Data indicate that increasing the Mach number from 0.70 to 0.95 caused the wing leading-edge vortex to burst over the wing when the wing was in the presence of the high canard. For some of the outboard span locations, the leading-edge vortex reattachment streamline intersects the wing trailing edge inboard of these span locations, thus, the Kutta condition was not satisfied. In general, the effect of adding a canard was to reduce the lift inboard and somewhat increase the lift outboard similar to the trends that would have been expected had the flow been attached.

17. Key Words (Suggested by Author(s))	18. Distribution Statement
close-coupled wing-canard transonic pressure distributions leading-edge vortex flow	Unclassified-Unlimited Star Category - 02

19. Security Classif. (of this report)	20. Security Classif. (of this page)	21. No. of Pages	22. Price*
Unclassified	Unclassified	9	$3.50

* For sale by the National Technical Information Service, Springfield Virginia 22161